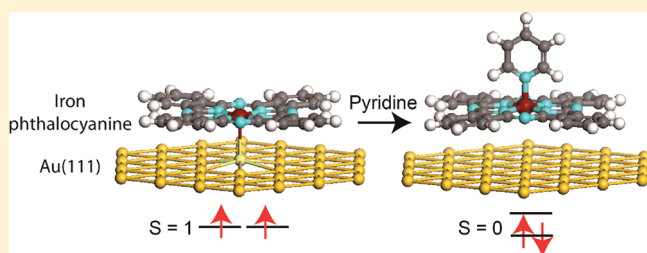


Pyridine Adsorption on Single-Layer Iron Phthalocyanine on Au(111)

Cristina Isvoranu,[†] Bin Wang,[§] Evren Ataman,[†] Karina Schulte,[‡] Jan Knudsen,[†] Jesper N. Andersen,[†] Marie-Laure Bocquet,[‡] and Joachim Schnadt^{*,†}[†]Division of Synchrotron Radiation Research, Department of Physics and [‡]MAX IV Laboratory, Lund University, Box 118, 221 00 Lund, Sweden[§]Laboratoire de chimie, Ecole normale supérieure de Lyon, 46, Allée d'Italie, 69364 Lyon Cedex 07, France

S Supporting Information

ABSTRACT: The adsorption of pyridine on monolayers of well-ordered, flat-lying iron phthalocyanine molecules on Au(111) is investigated by X-ray photoelectron spectroscopy, X-ray absorption spectroscopy, and density functional theory. It is found that pyridine both coordinates to the iron site of iron phthalocyanine and binds weakly to other sites. The iron coordination causes significant changes in the electronic structure of the iron phthalocyanine compound, with the implication of a change of the spin properties of the iron atoms due to the strong ligand field created by the pyridine axial ligand. Both low coverages and multilayer coverages of pyridine are considered. At low doses, the pyridine molecules are ordered, whereas in multilayers, no preferred orientation is observed. The orientation of the FePc molecules with respect to the Au(111) surface is not affected by the adsorption of pyridine.



INTRODUCTION

Because of their unique properties, phthalocyanines are among the most important macrocycle compounds. The macrocycles exhibit aromatic character, due to the planar structure consisting of a conjugated array of π electrons. As a consequence of their aromaticity, the molecules have high thermal and chemical stability,¹ and they are stable under electromagnetic radiation. For some metal phthalocyanines (such as Cu^{II}Pc, Co^{II}Pc, and Fe^{II}Pc, which is the main focus of this Article), the central metal ion is so strongly bonded that it can only be removed by breaking the macrocycle.² Such properties make metal phthalocyanines suitable candidates for ultrahigh vacuum (UHV) studies and also promising candidates for a large variety of technological applications. Their chemical properties can be varied by changing the metal ion in the center, by attaching different functional groups to the macrocycle, or, as will be shown in the present work, by ligand attachment to the central metal ion.

Phthalocyanine materials have become increasingly important because of the possibility of using them in a variety of technological fields. Applications comprise dye-sensitized solar cells,^{3,4} organic thin film transistors,^{5,6} organic light-emitting devices,^{7,8} fuel cells,^{9,10} catalysis,^{11–13} sensors,^{14–16} and photodynamic therapy.¹⁷ Gas adsorption on phthalocyanines is a subject worth studying from a fundamental point of view but also in connection to their possible catalytic and gas sensing properties and, as will be shown here, as an efficient way to change the spin properties of the iron ion.

In the present study, the interaction between the square planar iron phthalocyanine (FePc) molecule and the electron donor pyridine (Py) is studied (Figure 1). FePc was deposited onto a Au(111) single crystal at monolayer coverage, and different

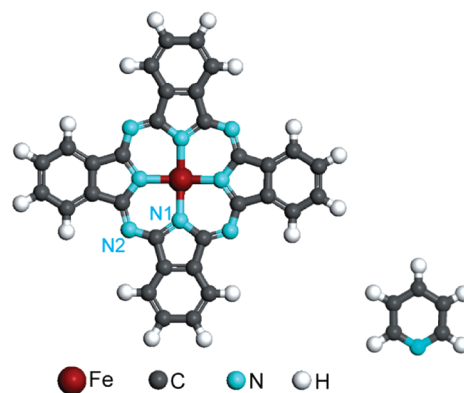


Figure 1. Molecular structure of the FePc and Py molecules.

amounts of Py were adsorbed under UHV conditions. X-ray absorption spectroscopy (XAS), X-ray photoelectron spectroscopy (XPS), and density functional theory (DFT) were used for characterization. We find that the electronic structure of FePc is affected significantly by the coordination of a Py axial ligand to the iron site of the macrocycle.

METHODS

The experiments were carried out at beamline I311¹⁸ of the Swedish national synchrotron radiation facility MAX-lab in

Received: May 12, 2011

Revised: September 6, 2011

Published: September 08, 2011

Lund. The beamline is equipped with a SCIENTA SES200 electron energy analyzer. The base pressure is in the high 10^{-11} mbar range. The Au(111) single crystal was cleaned by repeated cycles of sputtering and annealing. FePc monolayers were obtained by annealing thin FePc films obtained by vacuum sublimation onto a Au(111) substrate, which was kept at room temperature during deposition. The annealing temperature was around 380–400 °C; that is, it corresponded to the sublimation temperature of FePc. The sample was cooled to around –190 °C for performing the Py adsorption experiments. Prior to deposition, the FePc molecules (90% purity, Sigma-Aldrich) were degassed thoroughly for several days at temperatures slightly lower than the evaporation temperature. Directly before evaporation, the powder was further degassed by heating it to the evaporation temperature for approximately 3 to 4 h. The molecules were deposited from a resistively heated tantalum pocket that was brought to within 2 to 3 cm of the Au(111) sample. The tantalum pocket formed part of a molecule evaporator that was attached to the preparation chamber for the duration of the experiments. Py was dosed through a leak valve. The amount of gas adsorbed is quantified in Langmuirs (L), where $1 \text{ L} = 10^{-6} \text{ Torr} \times \text{s}$.

To avoid beam damage, we scanned the sample continuously during measurement. The scanning speed was adjusted as a result of test experiments on both the FePc/Au(111) and Py/FePc/Au(111) samples, in which the occurrence of beam damage was monitored. For the experiments, the sample scanning speed was set to a value ~ 3 to 4 times higher than the minimum speed required to avoid beam damage fully. Furthermore, the photoemission spectra were always recorded as single sweeps, meaning that each individual scan was inspected by eye to compare shapes and intensities before the scans were summed and the overall photoemission signal thus obtained. C 1s, N 1s, and Fe 2p photoemission spectra were recorded with photon energies of 385, 525, and 820 eV. The overall instrumental resolution ($\Delta E = (\Delta E_a^2 + \Delta E_{x\text{-ray}}^2)^{1/2}$, where ΔE_a is the energy resolution of the electron analyzer and $\Delta E_{x\text{-ray}}$ is that of the X-ray source) was 140 meV for the C 1s, 180 meV for the N 1s, and 280 meV for the Fe 2p photoemission spectra. All spectra were calibrated with respect to the Fermi level of the sample. A polynomial-type background was subtracted from the photoemission spectra, and all photoemission spectra shown were normalized with respect to the height of the most intense feature.

The N 1s XAS experiments were performed in Auger yield mode. The photon energy scale was calibrated by recording Au 4f photoemission spectra excited by first- and second-order light at relevant photon energies. The intensity of the XAS plots was corrected by dividing by the energy-dependent photon flux, which was recorded by measuring the photon-induced current on a photodiode placed behind the monochromator exit slit. Furthermore, a constant low-energy background was subtracted, and the spectra were then normalized to the step at ~ 25 eV above the adsorption edge.¹⁹ Two geometries were used, namely, grazing (65°) and normal photon incidence (0°) with respect to the sample normal.

Temperature-programmed XPS (TP-XPS) curves were recorded by measuring N 1s X-ray photoelectron spectra on the Py/FePc/Au(111) sample during heating. The sample was heated until Py had desorbed completely.

All DFT calculations were carried out with the VASP package,²⁰ using the PBE-GGA²¹ exchange-correction potential and the Ceperley–Alder version of the local density approximation

(LDA).^{22,23} Electron–core interactions were treated in the projector augmented wave approximation.^{24,25} We used an asymmetric slab with a four-layer (7×8) Au supercell as the substrate and the FePc positioned above the slab with its plane parallel to the slab surface. The Brillouin zone was sampled with a single k point at $\bar{\Gamma}$. The molecule and the uppermost Au layer were free to relax until the self-consistent forces reached 20 meV/Å. The cutoff energy was set to 400 eV. The method of Methfessel–Paxton was used to treat the partial occupancies (0.2 eV smearing width). The Au bulk lattice constant was kept fixed at the calculated value of the uncovered metal, $a = 4.17$ Å with GGA or 4.06 Å with LDA, both in good agreement with experimental values ($a = 4.08$ Å). The most stable configuration of FePc on Au(111) was determined by using both GGA and LDA functionals. Because the results from both functionals are very similar, the calculations shown in this Article refer to the PBE-GGA functional only. For the adsorption of Py, two geometries of the molecule were studied, one with the Py plane parallel to the N1–Fe–N1 line, and the second with the Py ring rotated along the z axis by 45°. (The plane is parallel to the N2–Fe–N2 line.) They were chosen on the basis of the fact that they are the only two geometries for which stabilizing hydrogen bond formation between the FePc nitrogen and pyridine hydrogen atoms seems feasible.

■ RESULTS AND DISCUSSION

Low Pyridine Doses. For the low dosage experiments, Py was adsorbed onto monolayers of FePc on Au(111) in increasing amounts, starting from 0.1 L and up to around 1.1 L. All FePc core levels are changed significantly as a result of the exposure of the sample to Py. Prior to Py adsorption, the N 1s photoemission line from the FePc molecules consists of a single peak located at 398.25 eV. Py adsorption results in two additional peaks on the high binding energy side of the N 1s peak of FePc (Figure 2), which shows that there exist at least two adsorption sites of Py. At the same time, the Fe 2p_{3/2} line becomes much narrower (Figure 3); the total full width at half-maximum (fwhm) of the monolayer Fe 2p_{3/2} signal is ~ 3.7 eV and it narrows to ~ 1.75 eV after Py adsorption. This shows clearly that one of the adsorption sites of Py on FePc is the iron ion and we suggest that adsorption occurs as coordination of the nitrogen lone pair orbital to the iron ion. The narrowing of the Fe 2p core-levels occurs up to a dose of 0.75 L, which is the “iron saturation dose”, at which all Fe sites in the FePc monolayer are bonded to Py. Higher Py doses are discussed below, but they did not result in any further change of the Fe 2p line. The fwhm at saturation as well as the overall changes of the Fe 2p spectra are very similar to what we have discussed thoroughly in a previous work concerned with the adsorption of ammonia on a monolayer of FePc on Au(111);²⁶ therefore, we do not go in detail here. In short, for the coordination of ammonia to the FePc iron ion, we found that the FePc molecules are decoupled from the substrate and that the local spin on the iron ion is quenched. In line with these previous results, we assign the narrowing of the Fe 2p line to the formation of a low-spin compound due to ligand field splitting^{26–29} and a partial decoupling of the FePc molecules from the Au(111) substrate. The fact that the NH₃ and Py ligands produce essentially the same effect is not surprising because the lone pair orbital on the N atom provides them with similar frontier orbital properties. Indeed, according to literature, both ligands are expected to produce similar ligand field splittings.³⁰ This leads to the same kind of electronic

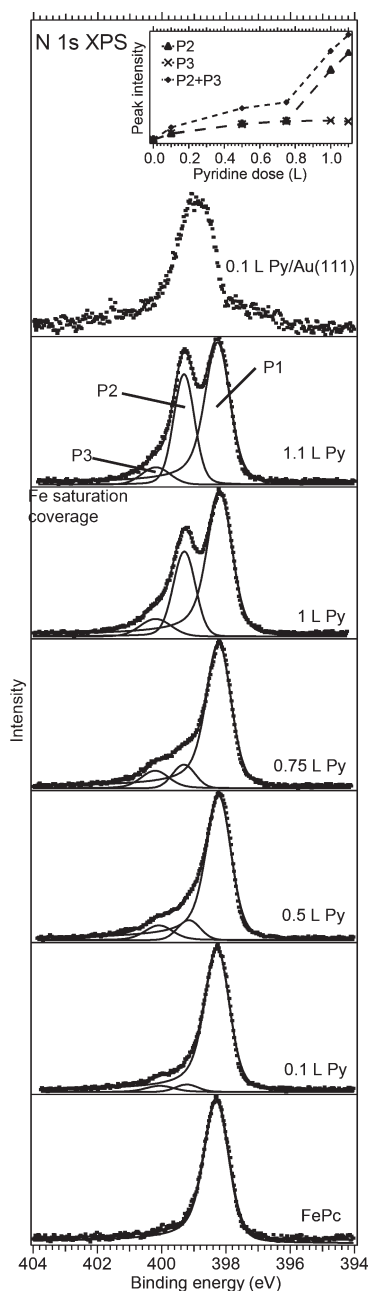


Figure 2. N 1s photoemission spectra (experimental data and least-squares fits) before and after adsorption of Py on monolayers of FePc on Au(111). The results show three peak components, P1, P2, and P3. The resulting spectrum after dosing 0.1 L of Py on bare Au(111) is also shown (top spectrum). The inset in Figure 2 shows the evolution of the N 1s Py peaks intensity (P2, P3, and the sum P2 + P3) as a function of Py dose.

redistribution of the d orbitals of the FePc iron ions, with similar changes of the valence spin as a result. Considering that the shape of the Fe 2p spectrum to a large degree is dictated by the influence of the valence spin on the photoemission process,^{31,32} it makes sense that both Py and NH₃ adsorption lead to the same width of the Fe 2p signal at saturation.

To determine the different Py species, we have performed least-squares fits of the N 1s spectra in Figure 2. Relevant peak parameters obtained from the fits are given in Table 1.

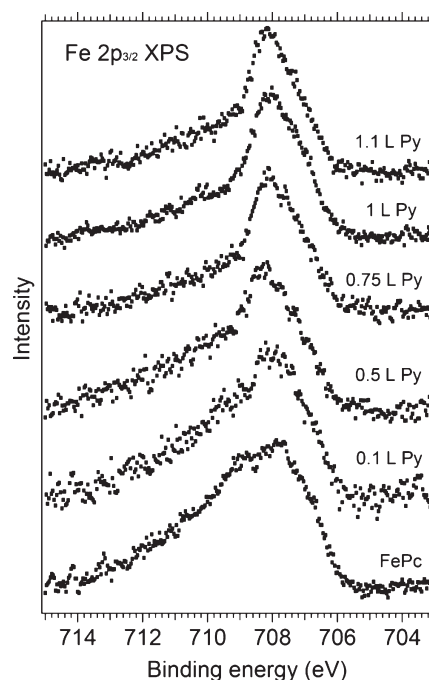


Figure 3. Fe 2p_{3/2} photoemission spectra before and after adsorption of increasing amounts of Py on a monolayer of FePc on Au(111). The spectra become significantly narrower after Py adsorption. Above 0.75 L, the spectra do not change anymore, indicating a saturation point where all Fe sites are bound to Py.

Table 1. Binding Energies in Electronvolts for the N 1s Photoemission Lines of FePc and Py and Relevant Peak Intensity Ratios As a Result of the Least-Squares Fits

Py amount (L)	binding energy (eV)			intensity ratio	
	P1	P2	P3	P3:P1	P3:P2
0.00	398.26 ± 0.05				
0.10	398.22 ± 0.05	399.19 ± 0.10	400.04 ± 0.05	1:23.1	1:1
0.50	398.18 ± 0.05	399.15 ± 0.10	400.08 ± 0.05	1:9.6	1:1
0.75	398.18 ± 0.05	399.30 ± 0.10	400.19 ± 0.05	1:8	1:1
1.00	398.15 ± 0.05	399.27 ± 0.05	400.18 ± 0.15	1:8	1:3.6
1.10	398.20 ± 0.05	399.30 ± 0.05	400.18 ± 0.15	1:8	1:4.9

The components are labeled P1, P2, and P3. P1 is due to photoemission from the nitrogen atoms of the FePc rings, P2 is assigned to Py molecules adsorbed in sites other than Fe and to Py molecules in the multilayer, and P3 is the spectral signature of Py molecules coordinated to Fe (Fe–N bonds), as can be deduced from the increase in this component up to the iron saturation dose, whereas it remains constant in intensity for higher doses (inset of Figure 2). Because the spectra are normalized to the height of P1, this clearly shows that the development of P3 is finished at saturation dose. The binding energy separation between P2 and P3 is ~0.9 eV. The binding energy changes of P2 and P3 with dose reported in Table 1 might be due to the uncertainty in estimating the binding energy. For P2, we estimate that the binding energy uncertainty is larger below saturation (±0.1 eV), whereas for P3, the uncertainty is larger above

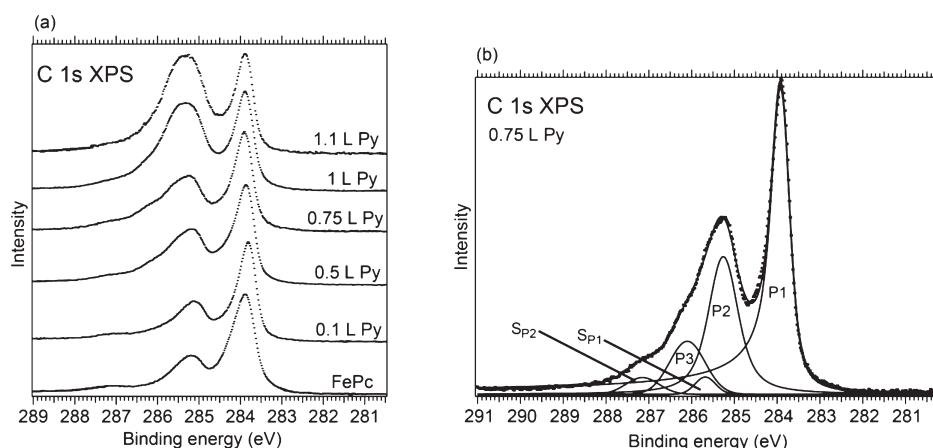


Figure 4. (a) C 1s photoemission spectra before and after the adsorption of increasing amounts of Py on the monolayer FePc/Au(111) and (b) the experimental data and the fit for the C 1s spectrum at the saturation coverage.

saturation (± 0.15 eV), when its intensity relative to that of P2 becomes reduced significantly.

The analysis of the N 1s peak intensity ratio is crucial in developing a better understanding of the nature of the adsorbed Py species. The P3:P1 intensity ratio is 1:8 at saturation dose (0.75 L), and it remains constant for higher doses. Above saturation (cf. the inset in Figure 2), P3 does not increase in intensity anymore. The 1:8 ratio is the expected stoichiometric ratio for the Fe-coordinated Py molecules, considering the formation of pentacoordinated complexes FePc(Py). In principle, hexacoordinated FePc(Py)₂ complexes could also be formed, but in the present case this is excluded because the Au(111) surface already plays the role of a sixth ligand to the iron ion. The size of the Py molecule makes it unlikely that it intercalates to a position in between the FePc compound and the support. (See also the XAS results below.)

P2 is present from the lowest doses of Py. Up to the saturation dose, the intensity ratio of P2 and P3 is 1:1, but above saturation, the intensity of P2 continues to increase, whereas P3 remains constant. Hence P2 is related to Py adsorption in sites other than Fe. Part of the intensity of P2 is related to the Py multilayer, as will be seen in the following section. Interestingly, the increase in intensity of the N 1s peak components related to (P2 + P3) is much more pronounced above saturation (inset of Figure 2), which implies that the Py sticking coefficient is larger above the saturation dose than below.

It is conceivable that the adsorption sites related to component P2 are sites on the Au(111) surface or on the benzene, pyrrole, or bridging nitrogen parts of the FePc compound. In Figure 2, we have included the N 1s spectrum for 0.1 L Py adsorbed on bare Au(111). It seems that at least a fraction of P2 might be due to a direct Py–Au(111) interaction. According to experimental^{33,34} and theoretical³⁵ studies, Py adsorption on metal surfaces has a dispersive character and can occur through the delocalized π system, through the N atom, or both. A closer look at the binding energies of the N 1s FePc peak shows that Py–pyrrole and Py–bridging nitrogen interactions cannot be neglected either. There is a slight decrease in the binding energy of the N 1s peak of FePc (P1) upon Py adsorption. In the case of FePc monolayers, the peak is centered at 398.26 eV, whereas after Py adsorption its binding energy varies between 398.22 and 398.15 eV. For Py amounts higher than 0.1 L, the P1 shift varies in between 0.06 and 0.11 eV. These values are larger than the

binding energy uncertainty, which suggests that the shift is real and should be attributed to Py/bridging nitrogen atoms and Py/pyrrole interactions. A corresponding shift was not observed for the adsorption of ammonia on FePc.²⁶ A third option for Py adsorption sites with contribution to P2 are the benzene rings of the FePc compound. If such interactions take place, then they are expected to be rather weak because no binding energy shift is observed in the C 1s core-levels arising from the benzene carbon atoms of FePc (the peak at ~ 284 eV in Figure 4). Py–benzene interactions are discussed in the literature; they have a combined dispersive and electrostatic character (van der Waals, hydrogen bond, dipole–dipole interaction), but there is no consensus about the predominance of electrostatic³⁶ or dispersive interactions.^{37,38} Unfortunately, from the available data, we are not able to point out exactly the adsorption sites giving rise to P2, and we are limited to discussing the possible options. In accordance with the discussion above, none of the mentioned possibilities can be excluded; indeed, it is likely that all sites play some role.

We have investigated the orientation of the Py molecules with respect to the FePc molecular plane by performing N 1s XAS experiments before and after adsorbing an the saturation dose of Py (Figure 5). It is known from previous studies^{26,39} that the FePc molecules at monolayer coverage are oriented with the molecular plane parallel to the Au(111) surface. In Figure 5, the π^* resonances situated in between 398 and 405 eV photon energy are shown. For the pristine FePc monolayer (Figure 5a), the π^* resonances have maximum intensity in grazing photon incidence (GI) and minimum intensity in normal photon incidence (NI). The opposite is true for the σ^* resonances (not shown here). The angular dependence of the FePc resonances, together with the knowledge that the π^* orbitals are perpendicular to the FePc macrocycle and the σ^* orbitals are in the plane of the macrocycle, prove a flat geometry of FePc on Au(111). The shape of the FePc resonances fits very well with previous data reported on FePc and other phthalocyanines on different metallic and semimetallic substrates.^{40–45}

When 0.75 L of Py is adsorbed (Figure 5b), a split of the lowest resonance into two components P1 and P2 is observed in GI geometry; in NI geometry, an additional π^* resonance P3 appears. Resonance P1, at ~ 398.4 eV has the same position as the LUMO of monolayer FePc/Au(111) observed in N 1s XAS. Resonances P2 and P3 at around 398.7 and 399.1 eV correspond

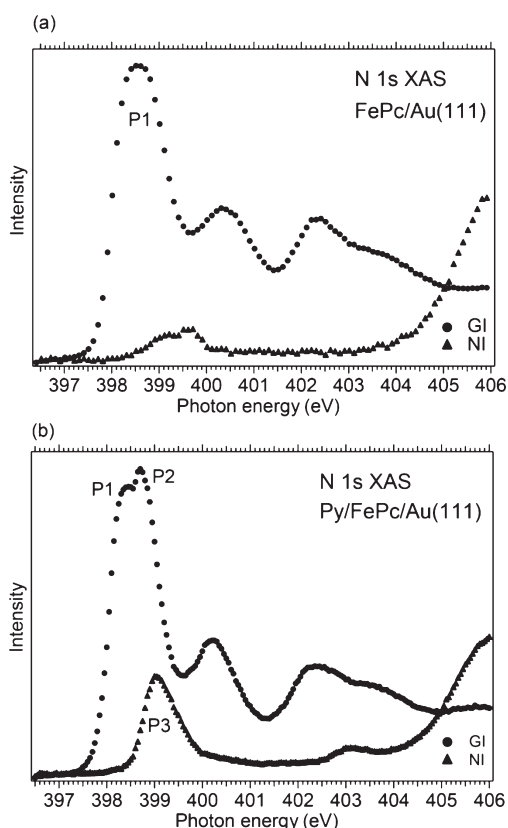


Figure 5. N 1s X-ray absorption spectra for (a) FePc/Au(111) and (b) Py/FePc/Au(111) with an amount of Py adsorbed equal to the iron saturation coverage (0.75 L). Two geometries were used for the experiments, grazing photon incidence (65° incidence) and normal photon incidence (0° incidence) with respect to the surface normal.

to the two different Py adsorption species. According to the photoemission results, Py coordinated to iron gives higher binding energy features than the Py adsorbed elsewhere on the sample. Translated into the XAS results, this implies that resonance P3 is due to Py coordinated to Fe and P2 to Py interacting with the FePc macrocycle interaction and possibly the Au(111) surface. Resonance P3 is present in NI only, and resonance P2 has maximum intensity in GI and vanishes in NI. This means the Py molecules coordinated to the iron ions adopt a standing geometry with respect to the FePc macrocycle, as opposed to the other Py species, which lie flat on sample at this particular Py coverage.

The C 1s X-ray photoemission spectra for increasing amounts of Py are shown in Figure 4a. The peak at ~ 285 eV grows with increasing amounts of Py. Figure 4b presents the results of least-squares curve fitting of the C 1s signal at iron saturation dose (0.75 L Py). There are five C 1s peak components: P1, P2, P3, S_{P1} , and S_{P2} . The binding energies are 283.88 for P1, 285.25 for P2, 286.1 for P3, 285.7 for S_{P1} , and 287.17 for S_{P2} . The P1, P2, S_{P1} , and S_{P2} components correspond to the peaks for the C 1s core levels of phthalocyanines.^{40,45–47} P1 and P2 are due to the photoemission from the benzene and pyrrole carbon atoms, respectively, and S_{P1} and S_{P2} are shakeup satellites of the main peaks P1 and P2. The intensity of P2 is, however, much larger than that expected from the number of pyrrole carbon atoms; that is, the P1/P2 ratio does not match the expected values from the stoichiometry of the FePc molecule, which shows that P2

contains additional contribution from the Py molecules. P2 is assigned to a mixed contribution from the FePc pyrrole carbon atoms and the carbon atoms of the Py molecules interacting with the macrocycle and/or the Au(111) surface (with the corresponding P2 component in the N 1s fits in Figure 2). P3 is assigned to photoemission from the carbon atoms of Py molecules coordinated to iron and is labeled as the corresponding N 1s component. The binding energy shift between the P2 and P3 C 1s components is 0.85 eV and is the same to within the uncertainty as the shift of 0.89 eV observed at saturation between the corresponding N 1s peaks.

Considering that the N 1s photoemission peak analysis shows that at saturation equal amounts of Py are adsorbed in the Fe site and in other sites, that is, on the macrocycle and possibly directly on the Au(111) surface, it is expected that the intensity ratio between the C 1s P2 and P3 peaks at saturation should be (number of pyrrole carbon atoms + number of Py carbon atoms)/(number of Py carbon atoms) = $(8 + 5):5$, that is, 2.6. This is indeed confirmed by an analysis of the components' intensities. The P1:P2 intensity ratio is instead underestimated. It is expected to be (number of benzene C atoms in FePc)/(number of pyrrole carbon atoms + number of Py carbon atoms) = $24:(8 + 5) = 1.84$, whereas the fit results give a ratio of only 1.53. This might be an indication that at this coverage Py molecules interacting with the macrocycle sit on top of the benzene rings, leading to an attenuation of the signal from the benzene carbon atoms but not the pyrrole ones. The explanation would also explain why a corresponding effect is not observed in the N 1s spectra.

It should be pointed out, however, that the analysis of the C 1s photoemission intensities is complicated by the fact that the pyridine C 1s line probably exhibits a chemical shift between the photoemission peaks from the different carbon atoms. Such a shift has been observed in photoemission from pyridine vapor.⁴⁸ As further discussed in the Supporting Information, on the basis of the present data set, we cannot exactly point out the position of these peaks, and thus we need to leave the issue of a finalized and complete analysis of the C 1s line open.

The DFT results for FePc/Au(111) and Py/FePc/Au(111) agree with the experimental findings. In the calculations of the Py/FePc/Au(111) system, we have limited ourselves to modeling the Fe-Py interaction. The main findings of the spectroscopy study, the coordination of Py to the iron center of FePc, spin quench caused by Py-Fe coordination, FePc-Au(111) decoupling upon Py adsorption, and geometry of the iron-coordinated Py molecules are all reproduced by the results of the DFT calculations (cf. Figure 6 for the geometry). All calculations were performed using the top configuration presented in Figure 6a, which was found to be the most stable FePc configuration on Au(111). (See the related discussion in ref 26.) Two geometries were considered for the adsorption of Py on FePc: the Py molecule along the N1–Fe–N1 direction and along the N2–Fe–N2 direction, respectively. The second geometry (Figure 6b) was found to be 0.16 eV more stable.

For FePc/Au(111), we have found previously²⁶ that a (weak) covalent bond is formed between the FePc iron atom and the Au(111) surface; this coupling is weakened by the adsorption of Py in the same way as by the adsorption of ammonia.¹¹ The magnetic moment of FePc/Au(111) calculated with the GGA functional is $2.36 \mu_B$, consistent with previous theoretical results.⁴⁹ As in the case of ammonia adsorption, Py quenches the spin on the iron atom and the magnetic moment after Py

adsorption is $\sim 0.25 \mu_B$. As in other recent publications, this shows that the adsorption of a ligand can be used to modify the magnetic properties of a surface organometallic compounds, either by directly affecting the metal atom's spin^{50,51} or by changing the system's magnetic anisotropy⁵² or the magnetic interaction with the support.⁵³ The spin quench is reversible: the spin of FePc can be recovered by desorption of Py. N 1s TP-XPS experiments after dosing 1 L of Py (Figure 7a) show that slowly heating the Py/FePc/Au(111) sample leads to the desorption of Py until the FePc signal is completely recovered and no Py signal is observed anymore. We have performed least-squares fits to all N 1s spectra of the TP-XPS scan. A detailed analysis of the variation of the intensity of the P2 component as a function of temperature shows that the desorption temperature of the P2 Py peak is -121°C (Figure 7b). The temperature is very close to -119°C reported for the desorption of bulk Py on Ag(111).⁵⁴ The low temperature suggests a weakly bonded Py species. We are not able to provide an analysis of the evolution of the P3 peak

intensity as a function of temperature because the intensity of P3, being already quite small (cf. Figure 2), is heavily affected by the relatively poor statistics of the TP-XPS spectra, which leads to large errors in estimating the intensity. The reason is the heating of the sample during the TP-XPS experiment, which only makes it possible to record a single sweep at each temperature. The desorption temperature for P3 (Fe–N) is higher, at around -90°C . From a Redhead analysis, it is estimated that the two desorption temperatures for the P2 and P3 components correspond to adsorption energies of -0.4 and -0.48 eV/molecule, respectively. Even if P2 and P3 show different adsorption energies, the N 1s photoemission spectra obtained for the stepped adsorption of Py (Figure 2) clearly show that both peaks are present already from very small doses of Py, which parallels the behavior of ammonia adsorption on FePc monolayers.²⁶ The reason for this somewhat extraordinary behavior still needs to be clarified.

High Pyridine Doses. In a second experiment series, multi-layer amounts of Py were adsorbed on the FePc/Au(111) sample. The Py coverage was increased to the point where thick Py multilayers were formed on top of FePc/Au(111) and no signal from the FePc molecules was observed anymore (after dosing 30 L of Py). The resulting N 1s, C 1s, and Fe 2p photoemission spectra are shown in Figure 8, and the N 1s binding energies obtained from curve fitting are provided in Table 2.

In the N 1s spectra, the intensity of the interface FePc (P1) and Py-Fe (P3) peaks becomes less intense gradually as the amount of Py is increased, whereas the P2 N 1s peak continues to increase in intensity (Figure 8a). This implies that P2 is not only due to interface Py species but also due to Py molecules in the multilayer. The same trend is observed in the C 1s spectra (Figure 8b). From Table 2, it is seen that the P2 N 1s multilayer peak is shifted by 0.85 eV to higher binding energies with respect to the peak at iron saturation dose; the same behavior is observed for the C 1s peak at ~ 285 eV. As expected, the shape of the Fe 2p spectra does not change with respect to the iron saturation dose. For metallic substrates, higher binding energies for multilayer coverages as compared with monolayer coverages are normal and can be explained by the improved core-hole screening by the support at low coverages. In the present case, the observed binding energy shift is most probably also caused by the reference

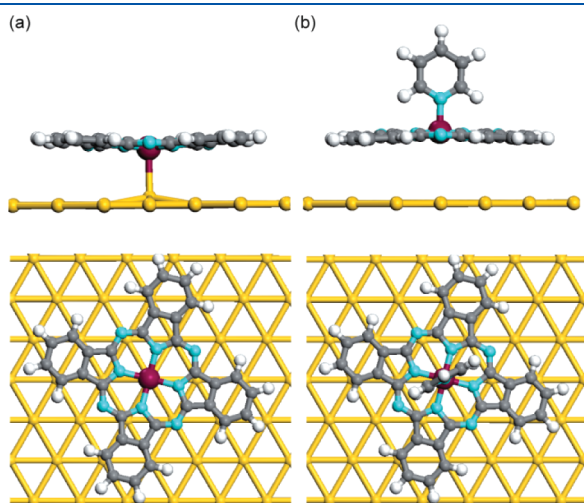


Figure 6. (a) Top and side views of the optimized structure of the most stable configuration of FePc on Au(111) from DFT with the GGA functional. An interaction between the Fe and the Au atom below is observed, with an Fe–Au distance of 2.76 Å. (b) Top and side views of the optimized structure of Py adsorbed on FePc/Au(111).

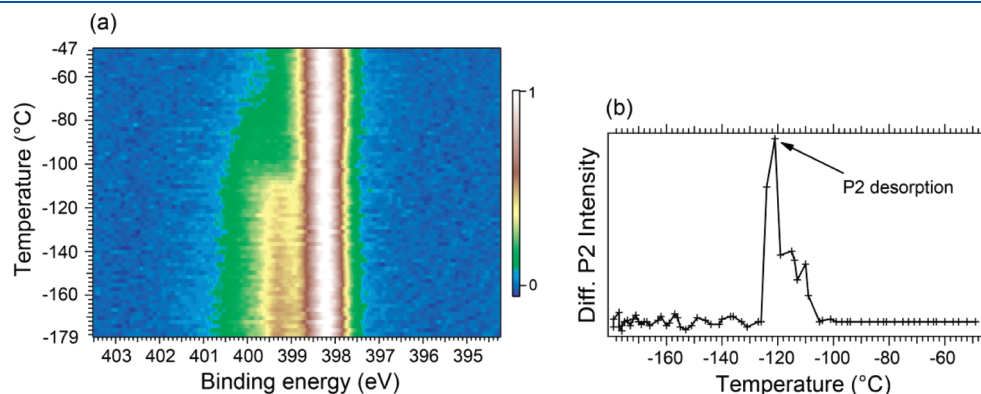


Figure 7. (a) N 1s TP-XPS experiments performed after adsorbing 1 L of Py on the FePc/Au(111) sample. The experiments involve heating the sample gradually to temperatures between -179 and -47°C up to complete desorption of Py and measuring N 1s photoemission spectra while heating. The color scale represents the intensity scale. Py starts desorbing around -126°C , and at around -85°C , all Py molecules are desorbed and the N 1s photoemission spectrum consists of the FePc signal only. (b) Differential of the intensity of P2 as a function of temperature, as obtained from the TP-XPS scans. The results show that P2 desorption takes place at -121°C .

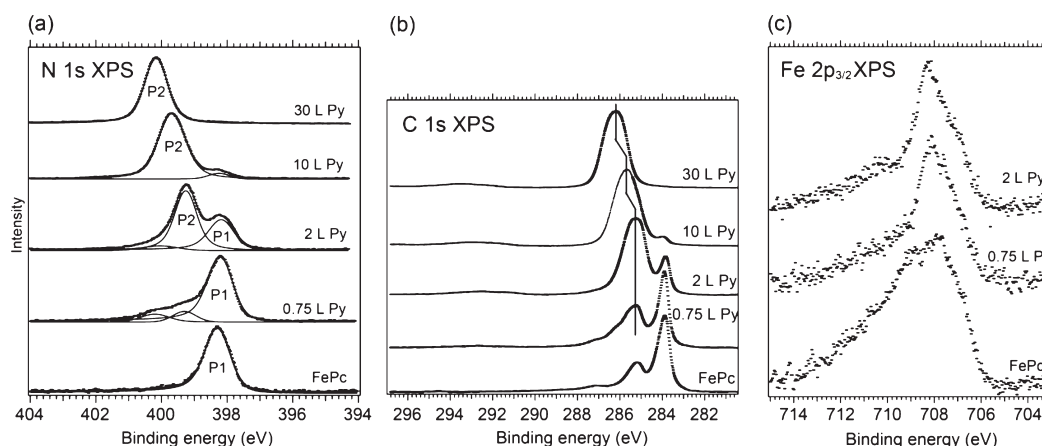


Figure 8. (a) N 1s, (b) C 1s, and (c) Fe 2p_{3/2} photoemission spectra before and after adsorbing Py on monolayers of FePc/Au(111) in amounts ranging from 2 to 30 L, where 30 L corresponds to thick Py multilayers. For comparison, the spectra at saturation (0.75 L) are also shown.

Table 2. Binding Energies for the N 1s Peak Components at High Py Doses As a Result Of the Least-Square Fits^a

Py amount (L)	binding energy (eV)		
	P1	P2	P3
0.00	398.26 ± 0.05		
0.75	398.18 ± 0.05	399.30 ± 0.10	400.19 ± 0.05
2.00	398.15 ± 0.05	399.25 ± 0.05	400.17 ± 0.15
10.00	398.18 ± 0.05	399.68 ± 0.05	
30.00		400.15 ± 0.05	

^aFor comparison, the binding energy of the N 1s peak obtained for a clean and saturated FePc monolayer is inserted.

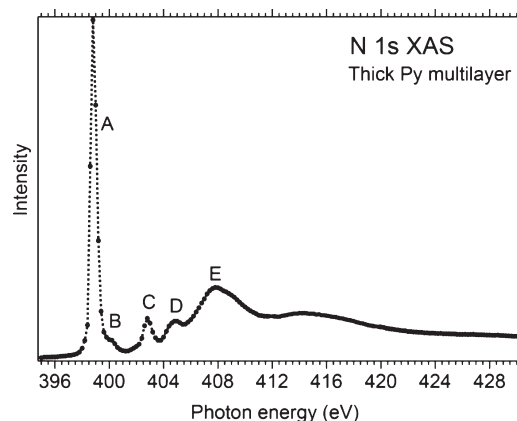


Figure 9. N 1s X-ray absorption spectrum of a thick multilayer of Py (30 L) grown on top of the FePc/Au(111) sample. The spectra were taken at an incidence angle of 65°. At this particular Py coverage, no signal was visible from the FePc macrocycle when measuring photoemission spectra.

level chosen for calibration. The vacuum level is the more appropriate reference level for weakly bound multilayers,⁵⁵ but it could not be determined because of experimental limitations. Instead, the calibration was carried out with respect to the Fermi level.

N 1s XAS experiments were performed on thick multilayers of Py (30 L) in both NI and GI geometry (Figure 9). The absorption spectra show no angular dependence of the resonances.

This shows that in thick multilayers Py does not have a preferred orientation with respect to the surface, but instead the layers are completely disordered. Because the spectra show no angular dependence, we show only the grazing incidence spectrum in Figure 9. There are several resonances, labeled A–E, whose positions fit well with previously reported data on gas phase Py:^{56,57} the most intense resonance A is at 398.8 eV, followed by a weak shoulder B at ~400.2 eV, resonance C at 402.8 eV, and resonances D and E at 404.8 eV and ~408 eV, respectively.

CONCLUSIONS

The adsorption of Py on FePc monolayer on Au(111) was studied for a broad range of coverages, starting at very low amounts and going up to thick multilayers of Py. Similar to our previous findings related to adsorption of ammonia on FePc, we find that Py adsorption quenches the local spin on the iron ion, which suggests the possibility of tailoring the magnetic properties of phthalocyanines by adsorption of molecular ligands. We also found that low doses of Py adsorb as two different species, one coordinated to the iron site of FePc and the second adsorbed elsewhere, either on FePc macrocycle or possibly interacting with the Au(111). Both Py species are present from the lowest coverages. At saturation, when all iron centers are bound to molecules, the iron-coordinated Py molecules adopt a perpendicular geometry with respect to the FePc rings, whereas the other Py species are flat. Above iron saturation coverage, the Py-Py sticking coefficient increases significantly, as shown by the intensity evolution of the N 1s peaks. As opposed to the low coverage situation, at multilayer coverage, the Py molecules are not ordered anymore; no preferred orientation is observed in this case.

ASSOCIATED CONTENT

S Supporting Information. C 1s X-ray photoelectron spectra obtained after adsorption of 0.1, 1, and 10 Langmuir of pyridine on bare Au(111). This material is available free of charge via the Internet at <http://pubs.acs.org>.

ACKNOWLEDGMENT

We are grateful to MAX-lab staff for technical support. The European Commission is acknowledged for financial support

through the Marie Curie Early Stage Researcher Training Network MONET, grant no. MEST-CT-2005-020908. We would also like to acknowledge Vetenskapsrådet (grant nos. 2004-4404 and 2010-5080) for funding.

REFERENCES

- (1) Milgrom, L. R. *The Colours of Life – An Introduction to the Chemistry of Porphyrins and Related Compounds*; Oxford University Press: New York, 1997.
- (2) Kadish, K. M.; Smith, K. M.; Guillard, R. *The Porphyrin Handbook: Phthalocyanines: Spectroscopic and Electrochemical Characterization*; Elsevier Science: San Diego, CA, 2003; Vol. 16.
- (3) Claessens, C. G.; Hahn, U.; Torres, T. *Chem. Rec.* **2008**, *8*, 75–97.
- (4) Riad, S. *Thin Solid Films* **2000**, *370*, 253–257.
- (5) de la Torre, G.; Claessens, C. G.; Torres, T. *Chem. Commun.* **2007**, *20*, 2000–2015.
- (6) Yuan, J.; Zhang, J.; Wang, J.; Yan, X.; Yan, D.; Xu, W. *Appl. Phys. Lett.* **2003**, *82*, 3967–3969.
- (7) Armstrong, N. R.; Wang, W.; Alloway, D. M.; Placencia, D.; Ratcliff, E.; Brumbach, M. *Macromol. Rapid Commun.* **2009**, *30*, 717–731.
- (8) Hohnholz, D.; Steinbrecher, S.; Hanack, M. *J. Mol. Struct.* **2000**, *521*, 231–237.
- (9) Baranton, S.; Coutanceau, C.; Roux, C.; Hahn, F.; Leger, J. M. *J. Electroanal. Chem.* **2005**, *577*, 223–234.
- (10) Zhao, F.; Harnisch, F.; Schröder, U.; Scholz, F.; Bogdanoff, P.; Herrmann, I. *Electrochem. Commun.* **2005**, *7*, 1405–1410.
- (11) Obirai, J. C.; Nyokong, T. *J. Electroanal. Chem.* **2007**, *600*, 251–256.
- (12) Lu, Y.; Reddy, R. G. *Int. J. Hydrogen Energy* **2008**, *33*, 3930–3937.
- (13) Kaliya, O. L.; Lukyanets, E. A.; Vorozhtsov, G. N. *J. Porphyrins Phthalocyanines* **1999**, *3*, 592–610.
- (14) Paoletti, A. M.; Pennesi, G.; Rossi, G.; Generosi, A.; Paci, B.; Albertini, V. R. *Sensors* **2009**, *9*, 5277–5297.
- (15) Spadavecchia, J.; Ciccarella, G.; Rella, R. *Sens. Actuators, B* **2005**, *106*, 212–220.
- (16) Palaniappan, A.; Mochhala, S.; Tay, F. E. H.; Su, X.; Phua, N. C. L. *Sens. Actuators, B* **2008**, *129*, 184–187.
- (17) Taquet, J. P.; Frochet, C.; Manneville, V.; Barberi-Heyob, M. B. *Curr. Med. Chem.* **2007**, *14*, 1673–1687.
- (18) Nyholm, R.; Andersen, J. N.; Johansson, U.; Jensen, B. N.; Lindau, I. *Nucl. Instrum. Methods Phys. Res., Sect. A* **2001**, *467*–468, 520–524.
- (19) Schnadt, J.; Schiessling, J.; O'Shea, J. N.; Gray, S. M.; Patthey, L.; Johansson, M. K. J.; Shi, M.; Krempaský, J.; Åhlund, J.; Karlsson, P. G.; Persson, P.; Mårtensson, N.; Brühwiler, P. A. *Surf. Sci.* **2003**, *540*, 39–54.
- (20) Kresse, G.; Furthmüller, J. *Phys. Rev. B* **1996**, *54*, 11169–11186.
- (21) Perdew, J. P.; Burke, K.; Ernzerhof, M. *Phys. Rev. Lett.* **1996**, *77*, 3865–3868.
- (22) Perdew, J. P.; Zunger, A. *Phys. Rev. B* **1981**, *23*, 5048–5079.
- (23) Ceperley, D. M.; Alder, B. J. *Phys. Rev. Lett.* **1980**, *45*, 566–569.
- (24) Blöchl, P. E. *Phys. Rev. B* **1994**, *50*, 17953–17979.
- (25) Kresse, G.; Joubert, D. *Phys. Rev. B* **1999**, *59*, 1758–1775.
- (26) Isvoranu, C.; Wang, B.; Ataman, E.; Schulte, K.; Knudsen, J.; Andersen, J. N.; Bocquet, M. L.; Schnadt, J. *J. Chem. Phys.* **2011**, *134*, 114710.
- (27) Cox, P. A. *The Electronic Structure and Chemistry of Solids*; Oxford Science Publications: New York, 1987.
- (28) Kotz, J. C.; Treichel, P. M.; Townsend, J. R. *Chemistry and Chemical Reactivity*; Thomson Brooks/Cole: Belmont, 2009.
- (29) Shriver, D. F.; Atkins, P. W.; Langford, C. H. *Inorganic Chemistry*; Oxford University Press: Oxford, U.K., 1994.
- (30) Figgis, B. N.; Hitchman, M. A. *Ligand Field Theory and its Applications*; Wiley-VCH: New York, 2000.
- (31) Weissenrieder, J.; Göthelid, M.; Månsson, M.; von Schenck, H.; Tjernberg, O.; Karlsson, U. O. *Surf. Sci.* **2003**, *527*, 163–172.
- (32) Sirotti, F.; Rossi, G. *Phys. Rev. B* **1994**, *49*, 15682–15687.
- (33) Demuth, J. E.; Christmann, K.; Sanda, P. N. *Chem. Phys. Lett.* **1980**, *76*, 201–206.
- (34) Hoon-Khosla, M.; Fawcett, W. R.; Chen, A.; Lipkowski, J.; Pettinger, B. *Electrochim. Acta* **1999**, *45*, 611–621.
- (35) Bilić, A.; Reimers, J. R.; Hush, N. S. *J. Phys. Chem. B* **2002**, *106*, 6740–6747.
- (36) Hohenstein, E. G.; Sherrill, C. D. *J. Phys. Chem. A* **2009**, *113*, 878–886.
- (37) Mignon, P.; Loverix, S.; De Proft, F. D.; Geerlings, P. *J. Phys. Chem. A* **2004**, *108*, 6038–6044.
- (38) Wang, W.; Hobza, P. *ChemPhysChem* **2008**, *9*, 1003–1009.
- (39) Cheng, Z. H.; Gao, L.; Deng, Z. T.; Liu, Q.; Jiang, N.; Lin, X.; He, X. B.; Du, S. X.; Gao, H. J. *J. Phys. Chem. C* **2007**, *111*, 2656–2660.
- (40) Isvoranu, C.; Åhlund, J.; Wang, B.; Ataman, E.; Mårtensson, N.; Puglia, C.; Andersen, J. N.; Bocquet, M. L.; Schnadt, J. *J. Chem. Phys.* **2009**, *131*, 214709.
- (41) Peisert, H.; Schwieger, T.; Auerhammer, J. M.; Knapfer, M.; Golden, M. S.; Fink, J.; Bressler, P. R.; Mast, M. *J. Appl. Phys.* **2001**, *90*, 466–469.
- (42) Biswas, I.; Peisert, H.; Casu, M. B.; Schuster, B.-E.; Nagel, P.; Merz, M.; Schuppler, S.; Chasse, T. *Phys. Status Solidi A* **2009**, *206*, 2524–2528.
- (43) Aristov, V. Y.; Molodtsova, O. V.; Maslyuk, V. V.; Vyalikh, D. V.; Zhilin, V. M.; Ossipyan, Y. A.; Bredow, T.; Mertig, I.; Knapfer, M. *J. Chem. Phys.* **2008**, *128*, 034703.
- (44) Kera, S.; Casu, M. B.; Schöll, A.; Schmidt, T.; Batchelor, D.; Rühl, E.; Umbach, E. *J. Chem. Phys.* **2006**, *125*, 014705.
- (45) Åhlund, J.; Nilson, K.; Schiessling, J.; Kjeldgaard, L.; Berner, S.; Mårtensson, N.; Puglia, C.; Brena, B.; Nyberg, M.; Luo, Y. *J. Chem. Phys.* **2006**, *125*, 034709.
- (46) Peisert, H.; Knapfer, M.; Fink, J. *Surf. Sci.* **2002**, *515*, 491–498.
- (47) Brena, B.; Luo, Y.; Nyberg, M.; Carniato, S.; Nilson, K.; Alfredsson, Y.; Åhlund, J.; Mårtensson, N.; Siegbahn, H.; Puglia, C. *Phys. Rev. B* **2004**, *70*, 195214.
- (48) Lucchini, S.; Thomas, T. D.; Børve, K. J.; Sæthre, L. J., **2011**, private communication.
- (49) Gao, L.; Ji, W.; Hu, Y. B.; Cheng, Z. H.; Deng, Z. T.; Liu, Q.; Jiang, N.; Lin, X.; Guo, W.; Du, S. X.; Hofer, W. A.; Xie, X. C.; Gao, H.-J. *Phys. Rev. Lett.* **2007**, *99*, 106402.
- (50) Wäckerlin, C.; Chylarecka, D.; Kleibert, A.; Müller, K.; Iacovita, C.; Nolting, F.; Jung, T. A.; Ballav, N. *Nat. Commun.* **2010**, *1*, 61.
- (51) Isvoranu, C.; Wang, B.; Schulte, K.; Ataman, E.; Knudsen, J.; Andersen, J. N.; Bocquet, M.-L.; Schnadt, J. *J. Phys.: Condens. Matter* **2010**, *22*, 472002.
- (52) Gambardella, P.; Stepanow, S.; Dmitriev, A.; Honolka, J.; de Groot, F. M. F.; Lingenfelder, M.; Gupta, S. S.; Sarma, D. D.; Bencok, P.; Stanescu, S.; Clair, S.; Pons, S.; Lin, N.; Seitsonen, A. P.; Brune, H.; Barth, J. V.; Kern, K. *Nat. Mater.* **2009**, *8*, 189.
- (53) Miguel, J.; Hermanns, C. F.; Bernien, M.; Krüger, A.; Kuch, W. *J. Phys. Chem. Lett.* **2011**, *2*, 1455.
- (54) Yang, M. C.; Rockey, T. J.; Pursell, D.; Dai, H. L. *J. Phys. Chem. B* **2001**, *105*, 11945–11948.
- (55) Chiang, T.-C.; Kaindl, G.; Mandel, T. *Phys. Rev. B* **1986**, *33*, 695–711.
- (56) Kolczewski, C.; Püttner, R.; Plashkevych, O.; Ågren, H.; Staemmler, V.; Martins, M.; Snell, G.; Schlachter, A. S.; Sant'Anna, M.; Kaindl, G.; Pettersson, L. G. M. *J. Chem. Phys.* **2001**, *115*, 6426–6437.
- (57) Hannay, C.; Duflo, D.; Flament, J.-P.; Hubin-Franskin, M.-J. *J. Chem. Phys.* **1999**, *110*, 5600–5610.